Estimation of Local Modeling Error and Goal-Oriented Adaptive Modeling of Heterogeneous Materials; Part I : Error Estimates and Adaptive Algorithms

J. Tinsley Oden and Kumar S. Vemaganti

Texas Institute for Computational and Applied Mathematics
The University of Texas at Austin,
Austin, Texas, USA
e–mail: {oden,kumar}@ticam.utexas.edu

Key words: Heterogeneous Materials, Hierarchical Modeling, Modeling Error, Local Error Estimates

Abstract. *A theory of a posteriori estimation of modeling errors in local quantities of interest in the analysis of heterogeneous elastic solids is presented. These quantities may, for example, represent averaged stresses on the surface of inclusions or mollifications of pointwise stresses or displacements, or, in general, local features of the "fine-scale" solution characterized by continuous linear functionals. These estimators are used to construct goal-oriented adaptive procedures in which models of the microstructure are adapted so as to deliver local features to a preset level of accuracy. Algorithms for implementing these procedures are discussed and preliminary numerical results are given.*

1   Introduction

The idea of automatically adapting characteristics of mathematical and computational models of heterogeneous media so as to obtain results of a specified level of accuracy was advanced in recent work on *hierarchical modeling* [11, 7]. In these papers, a posteriori bounds on the error in solutions to elastostatics problems induced by replacing fine-scale micromechanical properties by coarser scale or effective properties were derived in global energy norms. These error estimates were then used as a basis for an *adaptive modeling process* in which only enough fine-scale information sufficient to deliver results of a preset accuracy, measured in energy norms, is used to characterize the model. The resulting adaptive process can lead to significant computational savings, making possible the analysis of micromechanical effects in some cases that are intractable by traditional

approaches. Preliminary results on extensions of these adaptive approaches to a class of models depicting material damage were discussed in [6].

It is clear that adaptive procedures based on energy-norm estimates may be insensitive to very localized features of the fine-scale solution. Modeling error in characterizing average stresses on interfaces or on surfaces of inclusions, for example, may not be detected by energy-norm estimates unless virtually all of the fine-scale information is used in defining the computational/mathematical model. To efficiently control the accuracy of models of such local features, local estimates of modeling error are required.

In the present paper, we extend the theory of a posteriori modeling error estimation for heterogeneous materials to "quantities of interest", by which we mean local features of the response. In our theory, these quantities of interest could represent, for example, average stresses on material interfaces, boundary displacements, or mollified pointwise displacements, strains, or stresses. Mathematically, the quantities of interest are any feature of the fine-scale solution that can be characterized as continuous linear functionals on the space of functions to which the fine-scale solution belongs. We establish computable upper and lower bounds and sharp estimates of the errors in such quantities.

With local error estimates available, we develop *goal-oriented adaptive procedures*, in which the model is automatically adapted to deliver local quantities of interest to within a preset level of accuracy. These procedures are reminiscent of recently developed goal-oriented adaptive procedures for controlling numerical approximation error in linear functionals [8]. In the present investigation, we present an adaptive procedure that, in principle, utilizes only information on fine scale structures in a neighborhood of the local feature of interest sufficient to produce results of preset level of accuracy; information outside of this neighborhood need only reflect the response of models defined using effective, homogenized properties of the material.

Some basic features and assumptions underlying the approaches described here should be noted :

1. By an exact, fine-scale model, problem, or solution, we mean the exact solution $\mathbf{u}$ to a weak boundary value problem in elastostatics in which the elastic coefficients, characterized by a possibly rapidly varying elasticity tensor $\mathbf{E} = \mathbf{E}(\mathbf{x})$ which is known a priori. The modeling error $\mathbf{e}$ is the function defined as the difference between $\mathbf{u}$ and any coarse-scale solution $\tilde{\mathbf{u}}$ to an elastostatics problem defined on the same domain, subjected to the same external forces as the fine-scale problem, but with a different elasticity tensor $\tilde{\mathbf{E}}$ as coefficients in the problem : $\mathbf{e} = \mathbf{u} - \tilde{\mathbf{u}}$. The function $\tilde{\mathbf{u}}$, for example, could be the "homogenized solution" $\mathbf{u}^0$, the solution of the problem in which effective properties, characterized by a constant or piecewise constant "homogenized" elasticity tensor $\mathbf{E}^0$, are used.

2. In applications of our theory and algorithms, the coarse-scale solutions are generally computed using various numerical methods, such as finite elements. But estimation of numerical error is not considered in this paper; the techniques developed in [1, 8] can be used to control approximation error. Our concern here is *modeling error* in the sense discussed above, and this error can have quite different properties and behavior than numerical approximation error.

3. In theory, the tensor field $\mathbf{E}(\mathbf{x})$ defines at almost every point $\mathbf{x}$ in the body, an array $(E_{ijkl}(\mathbf{x}))$ with the standard ellipticity and symmetry properties. In our applications, $\mathbf{E}$ is generally piecewise constant, representing a so-called n-phase material with n isotropic phases, $n > 1$. For a large class of such materials, it is possible to represent the function $\mathbf{E}$ characterizing the fine-scale microstructure with sufficient accuracy using actual X-ray Computed Tomography (CT) imaging procedures with the overall model adaptivity package to characterize $\mathbf{E}$. The important details of this feature of adaptive modeling is the subject of a companion paper [10]. As will be seen later in this present paper, only CT-data sufficient to define $\mathbf{E} = \mathbf{E}(\mathbf{x})$ in local neighborhoods of features of interest are needed; the enormous data storage requirements of a global characterization of $\mathbf{E}$ called for in earlier global approaches are, in general, not needed in the goal-oriented adaptivity approaches advocated here.

4. It is important to emphasize that our goal is *not* to estimate effective properties of heterogeneous materials. Indeed, the familiar process of homogenization of fine-scale features of the coefficients is here only a mathematical artifact embedded in a broader computational strategy. Our error estimates and adaptive procedures apply to modeling errors in any kinematically admissible function, independent of the coefficients, so long as the underlying problem is well-posed. Nevertheless, the choice of approximations or regularizations of $\mathbf{E}$ will obviously affect modeling error and rates of convergence of the adaptive process to models delivering results with the target accuracies.

5. Extensions of our adaptive procedures to nonlinear problems are possible, although such extensions are not considered here. These extensions involve incorporating the goal-oriented adaptive process as an inner loop in a broader iterative process. In effect, such extensions amount to redefining the level of sophistication of the model used as a datum for error estimation.

In the section following this Introduction, we describe the model class of problems and lay down notations and preliminaries. We then establish a series of results on local estimates of errors in quantities of interest, including upper and lower bounds on errors.

This is followed by the description of a goal-oriented adaptive modeling algorithm. An analysis of the algorithm and results of preliminary numerical implementations are then presented. The detailed description of a computational environment designed to automate such procedures and the interface with imaging and visualization modules is the subject of forthcoming work [10].

2   Notations and Preliminaries

We consider an open bounded $\Omega \subset \mathbb{R}^N$, $N = 1, 2$, or 3, with boundary $\partial\Omega$. In general, Ω can be multi-connected and very irregular, but for present purposes, it suffices to take Ω to be Lipschitz with piecewise smooth boundaries. We denote by $H^m(\Omega), m \geq 0$, the space of functions with distributional derivatives of order $\leq m$ in $L^2(\Omega)$ and we use the notation $\mathbf{H}^m(\Omega) \overset{\text{def}}{=} (H^m(\Omega))^N$ and $\mathbf{L}^2(\Omega) \overset{\text{def}}{=} (L^2(\Omega))^N$.

The closure of Ω is the region occupied by a linearly elastic material body in static equilibrium under the action of body forces $\mathbf{f} \in \mathbf{L}^2(\Omega)$ and surface tractions $\mathbf{t} \in \mathbf{L}^2(\Gamma_t)$, with $\Gamma_t \subset \partial\Omega$. The displacements $\mathbf{u}$ of the body are prescribed as zero on $\Gamma_u = \partial\Omega \setminus \Gamma_t$. The space of admissible functions $\mathbf{V}(\Omega)$ is therefore defined as

$$\mathbf{V}(\Omega) \overset{\text{def}}{=} \left\{ \mathbf{v} : \mathbf{v} \in \mathbf{H}^1(\Omega), \mathbf{v}|_{\Gamma_u} = \mathbf{0} \right\}, \tag{1}$$

the boundary values being understood in the sense of traces of H^1-functions. In general, we will assume that meas $\Gamma_u > 0$; otherwise, our development is only altered by replacing $\mathbf{V}(\Omega)$ with $\mathbf{V}(\Omega) \setminus \mathbf{R}(\Omega)$, $\mathbf{R}(\Omega)$ being the linear space of infinitesimal rigid motions of the body.

The total potential energy of the body is characterized by the functional

$$\mathcal{J} : \mathbf{V}(\Omega) \to \mathbb{R}$$
$$\mathcal{J}(\mathbf{v}) \overset{\text{def}}{=} \tfrac{1}{2}\mathcal{B}(\mathbf{v}, \mathbf{v}) - \mathcal{F}(\mathbf{v}), \tag{2}$$

where $\mathcal{B}(\cdot, \cdot)$ is the symmetric, positive-definite, bilinear form,

$$\mathcal{B} : \mathbf{V}(\Omega) \times \mathbf{V}(\Omega) \to \mathbb{R}$$
$$\mathcal{B}(\mathbf{u}, \mathbf{v}) \overset{\text{def}}{=} \int_\Omega \boldsymbol{\nabla}\mathbf{v} : \mathbf{E}\,\boldsymbol{\nabla}\mathbf{u}\,\mathrm{d}\mathbf{x}, \tag{3}$$

and $\mathcal{F}(\cdot)$ is the linear functional,

$$\mathcal{F} : \mathbf{V}(\Omega) \to \mathbb{R}$$
$$\mathcal{F}(\mathbf{v}) \overset{\text{def}}{=} \int_\Omega \mathbf{f} \cdot \mathbf{v}\,\mathrm{d}\mathbf{x} + \int_{\Gamma_t} \mathbf{t} \cdot \mathbf{v}\,\mathrm{d}\mathbf{s} \tag{4}$$

4

It is also convenient to introduce the weighted inner product $((\cdot, \cdot))_E$ on $(L^2(\Omega))^{N^2} \times (L^2(\Omega))^{N^2}$ defined by

$$((\mathbf{A}, \mathbf{B}))_E \stackrel{\text{def}}{=} \int_\Omega \mathbf{A} : \mathbf{E}\,\mathbf{B}\,\mathrm{d}\mathbf{x} \tag{5}$$

for tensor fields $\mathbf{A}, \mathbf{B}$. Then, $\mathcal{B}(\mathbf{u}, \mathbf{v}) = ((\boldsymbol{\nabla}\mathbf{v}, \boldsymbol{\nabla}\mathbf{u}))_E$ and

$$((\boldsymbol{\nabla}\mathbf{v}, \boldsymbol{\nabla}\mathbf{v}))_E = \mathcal{B}(\mathbf{v}, \mathbf{v}) = \|\mathbf{v}\|_{E(\Omega)}^2, \tag{6}$$

where $\|\cdot\|_{E(\Omega)}$ is the *energy norm* of $\mathbf{v}$.

In (3), $\mathbf{E} \in (L^\infty(\Omega))^{N^2 \times N^2}$ is the uniformly elliptic tensor of elasticities which satisfies the standard symmetry conditions : $E_{ijkl}(\mathbf{x}) = E_{jikl}(\mathbf{x}) = E_{ijlk}(\mathbf{x}) = E_{klij}(\mathbf{x})$, for *a.e* $\mathbf{x}$ in $\Omega, 1 \leq i, j, k, l \leq N$. The notation $(:)$ denotes contraction of second order tensors ($\boldsymbol{\nabla}\mathbf{v} : \mathbf{E}\boldsymbol{\nabla}\mathbf{u} = v_{i,j}E_{ijkl}u_{k,l}$, summing on i, j, k, l, $v_{i,j} = \partial v_i/\partial x_j; u_{k,l} = \partial u_k/\partial x_l$). There, also, $\mathrm{d}\mathbf{x} = \mathrm{d}x_1\,\mathrm{d}x_2 \cdots \mathrm{d}x_N$ is the volume measure and $\mathrm{d}\mathbf{s}$ the surface element.

The material characterized by $\mathbf{E}$ is assumed to have a complex, not necessarily periodic microstructure so that $\mathbf{E}$ is a highly oscillatory function of position $\mathbf{x}$ over Ω.

2.1 The Fine-Scale Problem

Under the stated assumptions, the displacement field $\mathbf{u} \in \mathbf{V}(\Omega)$ that exists when the body is in static equilibrium under the action of external forces $(\mathbf{f}, \mathbf{t})$ is the unique admissible displacement that minimizes $\mathcal{J}$ over $\mathbf{V}(\Omega)$ and is the solution to the following weak boundary value problem :

$$\boxed{\begin{array}{c} \text{Find } \mathbf{u} \in \mathbf{V}(\Omega) \text{ such that} \\ \mathcal{B}(\mathbf{u}, \mathbf{v}) = \mathcal{F}(\mathbf{v}) \quad \forall\, \mathbf{v} \in \mathbf{V}(\Omega). \end{array}} \tag{7}$$

We shall refer to (7) as the *fine-scale problem* since it involves all the fine-scale features of the material, and to its solution $\mathbf{u}$ as the *fine-scale solution*. In the sense of distributions, (7) is equivalent to the elliptic system,

$$\begin{aligned} -\boldsymbol{\nabla} \cdot \boldsymbol{\sigma} &= \mathbf{f} \\ \boldsymbol{\sigma} &= \mathbf{E}\boldsymbol{\varepsilon} \\ 2\boldsymbol{\varepsilon} &= \boldsymbol{\nabla}\mathbf{u} + \boldsymbol{\nabla}\mathbf{u}^{\mathrm{T}} \\ \mathbf{u} &= \mathbf{0} \text{ on } \Gamma_u \\ \boldsymbol{\sigma} \cdot \mathbf{n} &= \mathbf{t} \text{ on } \Gamma_t, \end{aligned} \tag{8}$$

where $\mathbf{n}$ is the unit outward normal to $\partial\Omega$, and $\boldsymbol{\sigma}$ and $\boldsymbol{\varepsilon}$ are the stress and strain tensor fields, respectively.

2.2 The Regularized Problem

Various regularizations of problem (9) are obtained by replacing $\mathbf{E}$ by a regularized elasticity tensor. For example, if the microstructure is assumed to be periodic, it is common practice to replace $\mathbf{E}$ by a *homogenized elasticity tensor* $\mathbf{E}^0$, defining *effective properties* of the material, usually a constant tensor. For details on homogenization of periodic composites, see [4, 9]. Another approach used to regularize heterogeneous materials assumes the existence of a Representative Volume Element (RVE); see, for example, [3]. However, without restricting ourselves to a constant function, we assume that the elasticity tensor $\mathbf{E}$ is replaced by a suitable approximation $\mathbf{E}^0$ that satisfies the uniform ellipticity and symmetry conditions. We then can consider the *regularized* or *homogenized problem*,

$$\boxed{\begin{aligned} &\text{Find } \mathbf{u}^0 \in \mathbf{V}(\Omega) \text{ such that}\\ &\mathcal{B}^0(\mathbf{u}^0, \mathbf{v}) = \mathcal{F}(\mathbf{v}) \qquad \forall\, \mathbf{v} \in \mathbf{V}(\Omega) \end{aligned}} \tag{9}$$

where now

$$\mathcal{B}^0(\mathbf{u}^0, \mathbf{v}) \stackrel{\text{def}}{=} \int_\Omega \boldsymbol{\nabla} \mathbf{v} : \mathbf{E}^0 \boldsymbol{\nabla} \mathbf{u}^0 \, \mathrm{d}\mathbf{x}, \tag{10}$$

and $\mathcal{F}(\cdot)$ is again given by (4). The unique solution $\mathbf{u}^0$ to (9) is called the *regularized* or *homogenized solution*.

2.3 Review of Energy Estimates of the Modeling Error

The modeling error is defined as the difference between the fine-scale solution and the regularized solution

$$\mathbf{e}^0 \stackrel{\text{def}}{=} \mathbf{u} - \mathbf{u}^0. \tag{11}$$

We now review two results on the estimation of this error in the energy norm. For this purpose, we define

$$\mathcal{I}_0 = (\mathbf{I} - \mathbf{E}^{-1}\,\mathbf{E}^0), \tag{12}$$

where $\mathbf{I}$ is the identity tensor. Next, for $\mathbf{g} \in \mathbf{V}$, we define the associated linear *residual functional* $\mathcal{R}_{\mathbf{g}} : \mathbf{V}(\Omega) \to \mathbb{R}$,

$$\mathcal{R}_{\mathbf{g}}(\mathbf{v}) = -\int_\Omega \boldsymbol{\nabla} \mathbf{v} : \mathbf{E}\,\mathcal{I}_0 \boldsymbol{\nabla} \mathbf{g} \, \mathrm{d}\mathbf{x}, \quad \mathbf{v} \in \mathbf{V}(\Omega). \tag{13}$$

Theorem 2.1 *Let* $\mathbf{u}$ *and* $\mathbf{u}^0$ *be the solutions to problems (7) and (9) respectively. Then the following holds :*

$$\zeta_{\text{low}} \leq \|\mathbf{e}^0\|_{E(\Omega)} = \|\mathbf{u} - \mathbf{u}^0\|_{E(\Omega)} \leq \zeta_{\text{upp}}, \tag{14}$$

where

$$\zeta_{\text{low}} \stackrel{\text{def}}{=} \frac{|\mathcal{R}_{\mathbf{u}^0}(\mathbf{u}^0)|}{\|\mathbf{u}^0\|_{E(\Omega)}}, \quad \zeta_{\text{upp}} \stackrel{\text{def}}{=} \left(\left(\mathcal{I}_0 \boldsymbol{\nabla} \mathbf{u}^0, \mathcal{I}_0 \boldsymbol{\nabla} \mathbf{u}^0 \right) \right)_E^{1/2}. \tag{15}$$

$\square$

For proofs, see [11] and [5]. Both assertions follow from the fact that the modeling error $\mathbf{e}^0$ is governed by

$$\mathcal{B}(\mathbf{e}^0, \mathbf{v}) = \mathcal{R}_{\mathbf{u}^0}(\mathbf{v}), \ \forall \, \mathbf{v} \, \in \, \mathbf{V}(\Omega). \tag{16}$$

Using the above result, it is possible to estimate the energy norm of the difference between the fine-scale solution $\mathbf{u}$ and any admissible function $\mathbf{z} \in \mathbf{V}(\Omega)$.

Corollary 2.1 *Let* $\mathbf{u}$ *and* $\mathbf{u}^0$ *be the solutions to problems (7) and (9), respectively, and let* $\mathbf{z} \in \mathbf{V}(\Omega) \setminus \{\mathbf{0}\}$. *Then,*

$$\zeta_{\text{low}}^z \leq \|\mathbf{u} - \mathbf{z}\|_{E(\Omega)} \leq \zeta_{\text{upp}}^z, \tag{17}$$

where

$$\zeta_{\text{low}}^z \stackrel{\text{def}}{=} \frac{|\mathcal{F}(\mathbf{z}) - \mathcal{B}(\mathbf{z}, \mathbf{z})|}{\|\mathbf{z}\|_{E(\Omega)}}, \quad \zeta_{\text{upp}}^z \stackrel{\text{def}}{=} \sqrt{2(\mathcal{J}(\mathbf{z}) - \mathcal{J}(\mathbf{u}^0)) + \zeta_{\text{upp}}^2}, \tag{18}$$

with $\mathcal{J}$ *as defined in (2) and* ζ_{upp} *as defined in (15).*

Proof. The proof for the assertion $\|\mathbf{u} - \mathbf{z}\|_{E(\Omega)} \leq \zeta_{\text{upp}}^z$ can be found in [7]. For the lower bound, we have

$$\mathcal{B}(\mathbf{u} - \mathbf{z}, \mathbf{v}) = \mathcal{F}(\mathbf{v}) - \mathcal{B}(\mathbf{z}, \mathbf{v}) \ \forall \ \mathbf{v} \in \mathbf{V}(\Omega). \tag{19}$$

Then, it is straightforward to show that

$$\|\mathbf{u} - \mathbf{z}\|_{E(\Omega)} = \sup_{\mathbf{v} \in \mathbf{V}(\Omega) \setminus \{\mathbf{0}\}} \frac{|\mathcal{F}(\mathbf{v}) - \mathcal{B}(\mathbf{z}, \mathbf{v})|}{\|\mathbf{v}\|_{E(\Omega)}}, \tag{20}$$

and by picking $\mathbf{v} = \mathbf{z}$, we obtain

$$\|\mathbf{u} - \mathbf{z}\|_{E(\Omega)} \geq \frac{|\mathcal{F}(\mathbf{z}) - \mathcal{B}(\mathbf{z}, \mathbf{z})|}{\|\mathbf{z}\|_{E(\Omega)}}, \tag{21}$$

which concludes the proof. $\square$

3 Modeling Error in Local Quantities of Interest

As mentioned in the Introduction, global estimates of modeling error, such as the energy estimate presented in Theorem 2.1, can be insensitive to local quantities of interest such as interfacial stresses. To address this problem, we now present a theory for the estimation of modeling error in quantities of interest that can be characterized as continuous linear functionals on the space of admissible functions $\mathbf{V}(\Omega)$. This theory represents a significant departure from more traditional theories of error estimation in that it allows the estimation of modeling error in virtually any quantity of interest to the analyst, such as (mollified) pointwise values of stresses and displacements, boundary displacements and averaged stresses. Concrete examples of such quantities of interest will be given in the section on numerical experiments.

The goal in this section is to obtain bounds on the quantity $L(\mathbf{u}) - L(\mathbf{u}^0) = L(\mathbf{e}^0)$, where $L \in \mathbf{V}^{'}(\Omega)$ is a continuous linear functional. We first present a result on obtaining upper and lower bounds on $L(\mathbf{e}^0)$. Next, we show how this theory can be extended to obtain bounds on the error in *arbitrary admissible* functions $\mathbf{z} \in \mathbf{V}(\Omega)$, i.e., bounds on the quantity $L(\mathbf{u}) - L(\mathbf{z}) = L(\mathbf{u} - \mathbf{z})$, where $\mathbf{z}$ is not necessarily the solution to an elastostatics problem posed on the domain Ω. The motivation behind this is that the modeling error in local quantities of interest can often be reduced by adding perturbations to the regularized solution such that the sum is still an admissible function.

3.1 Upper and Lower Bounds on Modeling Errors in Local Quantities of Interest

Let L be a continuous linear functional on $\mathbf{V}(\Omega)$, $L \in \mathbf{V}^{'}(\Omega)$. As a first step, we first pose the following global *adjoint fine-scale problem* :

$$\boxed{\begin{array}{c} \text{Find } \mathbf{w} \in \mathbf{V}(\Omega) \text{ such that} \\ \mathcal{B}(\mathbf{v}, \mathbf{w}) = L(\mathbf{v}) \qquad \forall\, \mathbf{v} \in \mathbf{V}(\Omega) \end{array}} \qquad (22)$$

The solution $\mathbf{w}$ to the adjoint fine-scale problem is referred to as the *fine-scale influence function*. The regularized version of this problem is referred to as the *adjoint regularized problem* and reads

$$\boxed{\begin{array}{c} \text{Find } \mathbf{w}^0 \in \mathbf{V}(\Omega) \text{ such that} \\ \mathcal{B}^0(\mathbf{v}, \mathbf{w}^0) = L(\mathbf{v}) \qquad \forall\, \mathbf{v} \in \mathbf{V}(\Omega). \end{array}} \qquad (23)$$

The solution to this problem will be referred to as the *regularized influence function*. In what follows, we sometimes refer to the problems (7) and (9) as the *primal fine-scale*

problem and *primal regularized problem*, respectively. It is obvious that, under the stated assumptions on $\mathbf{E}$ and $\mathbf{E}^0$, the functions $\mathbf{w}$ and $\mathbf{w}^0$ exist and are uniquely defined.

It immediately follows that the modeling error in the influence function

$$\bar{\mathbf{e}}^0 \stackrel{\text{def}}{=} \mathbf{w} - \mathbf{w}^0 \tag{24}$$

satisfies (recall (16))

$$\mathcal{B}(\mathbf{v}, \bar{\mathbf{e}}^0) = \mathcal{R}_{\mathbf{w}^0}(\mathbf{v}) \qquad \forall\, \mathbf{v} \in \mathbf{V}(\Omega). \tag{25}$$

We also note that $\bar{\mathbf{e}}^0$ satisfies the following relationship (analogous to (14)) :

$$\bar{\zeta}_{\text{low}} \leq \|\bar{\mathbf{e}}^0\|_{E(\Omega)} = \|\mathbf{w} - \mathbf{w}^0\|_{E(\Omega)} \leq \bar{\zeta}_{\text{upp}} \tag{26}$$

where

$$\bar{\zeta}_{\text{low}} \stackrel{\text{def}}{=} \frac{|\mathcal{R}_{\mathbf{w}^0}(\mathbf{w}^0)|}{\|\mathbf{w}^0\|_{E(\Omega)}}; \quad \bar{\zeta}_{\text{upp}} \stackrel{\text{def}}{=} \left(\left(\mathcal{I}_0 \boldsymbol{\nabla} \mathbf{w}^0, \mathcal{I}_0 \boldsymbol{\nabla} \mathbf{w}^0 \right) \right)_E^{1/2}. \tag{27}$$

We now state the main result on the estimation of modeling error in quantities of interest :

Theorem 3.1 *Let $\mathbf{u}^0$ and $\mathbf{w}^0$ be the solutions to problems (9) and (23), respectively. Then,*

$$\eta_{\text{low}} \leq L(\mathbf{e}^0) \leq \eta_{\text{upp}} \tag{28}$$

where

$$\eta_{\text{low}} \stackrel{\text{def}}{=} \frac{1}{4}(\eta_{\text{low}}^+)^2 - \frac{1}{4}(\eta_{\text{upp}}^-)^2 + \mathcal{R}_{\mathbf{u}^0}(\mathbf{w}^0), \tag{29}$$

$$\eta_{\text{upp}} \stackrel{\text{def}}{=} \frac{1}{4}(\eta_{\text{upp}}^+)^2 - \frac{1}{4}(\eta_{\text{low}}^-)^2 + \mathcal{R}_{\mathbf{u}^0}(\mathbf{w}^0), \tag{30}$$

with arbitrary $s \in \mathbb{R}^+$,

$$\eta_{\text{upp}}^{\pm} \stackrel{\text{def}}{=} \sqrt{s^2 \zeta_{\text{upp}}^2 \pm 2\left(\left(\mathcal{I}_0 \boldsymbol{\nabla} \mathbf{u}^0, \mathcal{I}_0 \boldsymbol{\nabla} \mathbf{w}^0 \right) \right)_E + s^{-2} \bar{\zeta}_{\text{upp}}^2}, \tag{31}$$

and

$$\eta_{\text{low}}^{\pm} \stackrel{\text{def}}{=} \frac{|\mathcal{R}_{s\mathbf{u}^0 \pm s^{-1}\mathbf{w}^0}(\mathbf{u}^0 + \theta^{\pm}\mathbf{w}^0)|}{\|\mathbf{u}^0 + \theta^{\pm}\mathbf{w}^0\|_{E(\Omega)}}, \tag{32}$$

where ζ_{upp} and $\bar{\zeta}_{\text{upp}}$ are defined by (15) and (27), respectively, and $\theta^{\pm}$ is given by

$$\theta^{\pm} = \frac{\mathcal{B}(\mathbf{u}^0, \mathbf{w}^0)\mathcal{R}_{\mathbf{u}^0}(s\mathbf{u}^0 \pm s^{-1}\mathbf{w}^0) - \mathcal{B}(\mathbf{u}^0, \mathbf{u}^0)\mathcal{R}_{\mathbf{w}^0}(s\mathbf{u}^0 \pm s^{-1}\mathbf{w}^0)}{\mathcal{B}(\mathbf{u}^0, \mathbf{w}^0)\mathcal{R}_{\mathbf{w}^0}(s\mathbf{u}^0 \pm s^{-1}\mathbf{w}^0) - \mathcal{B}(\mathbf{w}^0, \mathbf{w}^0)\mathcal{R}_{\mathbf{u}^0}(s\mathbf{u}^0 \pm s^{-1}\mathbf{w}^0)}. \tag{33}$$

Proof. The outline of the proof is given below; see [5] for details. The error in the quantity of interest can be decomposed as

$$L(\mathbf{e}^0) = \mathcal{B}(\mathbf{e}^0, \mathbf{w}) = \mathcal{B}(\mathbf{e}^0, \bar{\mathbf{e}}^0) + \mathcal{B}(\mathbf{e}^0, \mathbf{w}^0) = \mathcal{B}(s\mathbf{e}^0, s^{-1}\bar{\mathbf{e}}^0) + \mathcal{R}_{\mathbf{u}^0}(\mathbf{w}^0), \qquad (34)$$

where $s \in \mathbb{R}^+$ is an, as yet, unspecified positive scaling factor. Now, using a simple property of an inner product, we rewrite the expression (34) as

$$L(\mathbf{e}^0) = \frac{1}{4}\|s\mathbf{e}^0 + s^{-1}\bar{\mathbf{e}}^0\|_{E(\Omega)}^2 - \frac{1}{4}\|s\mathbf{e}^0 - s^{-1}\bar{\mathbf{e}}^0\|_{E(\Omega)}^2 + \mathcal{R}_{\mathbf{u}^0}(\mathbf{w}^0). \qquad (35)$$

The first two terms on the right hand side of (35) can be bounded above by noting that the quantity $s\mathbf{e}^0 \pm s^{-1}\bar{\mathbf{e}}^0$ satisfies

$$\mathcal{B}(s\mathbf{e}^0 \pm s^{-1}\bar{\mathbf{e}}^0, \mathbf{v}) = \mathcal{R}_{s\mathbf{u}^0 \pm s^{-1}\mathbf{w}^0}(\mathbf{v}) \quad \forall \, \mathbf{v} \in \mathbf{V}(\Omega), \qquad (36)$$

and hence

$$\|s\mathbf{e}^0 \pm s^{-1}\bar{\mathbf{e}}^0\|_{E(\Omega)} \le \eta_{\text{upp}}^{\pm}, \qquad (37)$$

with,

$$\begin{aligned}
\eta_{\text{upp}}^{\pm} &\overset{\text{def}}{=} \left\{ \int_\Omega \mathcal{I}_0 \boldsymbol{\nabla}(s\mathbf{u}^0 \pm s^{-1}\mathbf{w}^0) : \mathbf{E}\,\mathcal{I}_0 \boldsymbol{\nabla}(s\mathbf{u}^0 \pm s^{-1}\mathbf{w}^0)\,\mathrm{d}\mathbf{x} \right\}^{1/2} \\
&= \left\{ s^2 \zeta_{\text{upp}}^2 \pm 2((\mathcal{I}_0 \boldsymbol{\nabla}\mathbf{u}^0, \mathcal{I}_0 \boldsymbol{\nabla}\mathbf{w}^0))_E + s^{-2}\bar{\zeta}_{\text{upp}}^2 \right\}^{1/2}.
\end{aligned} \qquad (38)$$

To obtain a lower bound on the quantity $s\mathbf{e}^0 \pm s^{-1}\bar{\mathbf{e}}^0$, we note that

$$\|s\mathbf{e}^0 \pm s^{-1}\bar{\mathbf{e}}^0\|_{E(\Omega)} = \|\mathcal{R}_{s\mathbf{u}^0 \pm s^{-1}\mathbf{w}^0}\|_{E'(\Omega)} \ge \frac{|\mathcal{R}_{s\mathbf{u}^0 \pm s^{-1}\mathbf{w}^0}(\mathbf{v})|}{\|\mathbf{v}\|_{E(\Omega)}}, \qquad (39)$$

for any $\mathbf{v} \in \mathbf{V}(\Omega) \setminus \{\mathbf{0}\}$. A linear combination of $\mathbf{u}^0$ and $\mathbf{w}^0$ of the form $\mathbf{v} = \mathbf{u}^0 + \theta^{\pm}\mathbf{w}^0$, $\theta^{\pm} \in \mathbb{R}$, is then used in the above expression to obtain the best possible lower bound. The value $\theta^{\pm}$ is found by a simple extremization process. The third term $\mathcal{R}_{\mathbf{u}^0}(\mathbf{w}^0)$ depends only on known quantities. $\qquad \square$

It can be shown that the optimal value of the scaling factor s is given by $s^* = \sqrt{\|\bar{\mathbf{e}}^0\|_{E(\Omega)}/\|\mathbf{e}^0\|_{E(\Omega)}}$. However, since $\bar{\mathbf{e}}^0$ and $\mathbf{e}^0$ are not known exactly, we use $s^* = \sqrt{\bar{\zeta}_{\text{upp}}/\zeta_{\text{upp}}}$. Also, in our numerical experiments, we employ the following *estimates* of the modeling error in the quantity of interest :

$$L(\mathbf{e}^0) \approx \eta_{\text{est,upp}} \overset{\text{def}}{=} \frac{1}{4}(\eta_{\text{upp}}^+)^2 - \frac{1}{4}(\eta_{\text{upp}}^-)^2 + \mathcal{R}_{\mathbf{u}^0}(\mathbf{w}^0), \qquad (40)$$

and

$$L(\mathbf{e}^0) \approx \eta_{\text{est,low}} \stackrel{\text{def}}{=} \frac{1}{4}(\eta_{\text{low}}^+)^2 - \frac{1}{4}(\eta_{\text{low}}^-)^2 + \mathcal{R}_{\mathbf{u}^0}(\mathbf{w}^0). \tag{41}$$

An important feature of the theorem above is that the elasticity tensor $\mathbf{E}^0$ need not be a constant function; it need only satisfy the uniform ellipticity and symmetry conditions.

3.2   Modeling Error in Quantities of Interest for Admissible Functions

We now demonstrate how to obtain bounds on the quantity $L(\mathbf{u} - \mathbf{z})$ for admissible functions $\mathbf{z} \in \mathbf{V}(\Omega), \mathbf{z} \neq \mathbf{0}$, where $\mathbf{L} \in \mathbf{V}'(\Omega)$ denotes a quantity of interest. We first define, for $s \in \mathbb{R}^+$, the functional $\mathcal{J}_s^\pm : \mathbf{V}(\Omega) \to \mathbb{R}$,

$$\mathcal{J}_s^\pm(\mathbf{v}) \stackrel{\text{def}}{=} \frac{1}{2}\mathcal{B}(\mathbf{v}, \mathbf{v}) - (s\mathcal{F} \pm s^{-1}L)(\mathbf{v}), \ \ \mathbf{v} \in \mathbf{V}(\Omega). \tag{42}$$

It is easy to see that :

- The functional $\mathcal{J}_s^\pm$ has a unique minimizer $\boldsymbol{\chi}_s^\pm$ that satisfies

$$\mathcal{B}(\boldsymbol{\chi}_s^\pm, \mathbf{v}) = (s\mathcal{F} \pm s^{-1}L)(\mathbf{v}), \ \ \forall \ \mathbf{v} \in \mathbf{V}(\Omega). \tag{43}$$

  Moreover,

$$\boldsymbol{\chi}_s^\pm \equiv s\mathbf{u} \pm s^{-1}\mathbf{w}, \tag{44}$$

  where $\mathbf{u}$ is the unique solution to (7) and $\mathbf{w}$ is the unique solution to (22).

- If $\mathbf{v} \in \mathbf{V}(\Omega), \mathbf{v} \neq \mathbf{0}$, then, in the spirit of Corollary 2.1, we have

$$\eta_{\text{low}}^\pm(\mathbf{v}) \leq \|(s\mathbf{u} \pm s^{-1}\mathbf{w}) - \mathbf{v}\|_{E(\Omega)} = \|\boldsymbol{\chi}_s^\pm - \mathbf{v}\|_{E(\Omega)} \leq \eta_{\text{upp}}^\pm(\mathbf{v}), \tag{45}$$

  where,

$$\eta_{\text{upp}}^\pm(\mathbf{v}) \stackrel{\text{def}}{=} \sqrt{2\left(\mathcal{J}_s^\pm(\mathbf{v}) - \mathcal{J}_s^\pm(s\mathbf{u}^0 \pm s^{-1}\mathbf{w}^0)\right) + (\eta_{\text{upp}}^\pm)^2}, \tag{46}$$

  and

$$\eta_{\text{low}}^\pm(\mathbf{v}) \stackrel{\text{def}}{=} \frac{|(s\mathcal{F} \pm s^{-1}L)(\mathbf{v}) - \mathcal{B}(\mathbf{v}, \mathbf{v})|}{\|\mathbf{v}\|_{E(\Omega)}}, \tag{47}$$

  where $\eta_{\text{upp}}^\pm$ is as defined in (31).

11

These preliminaries bring us to the following result :

Theorem 3.2 *Let $\mathbf{u}^0$ and $\mathbf{w}^0$ be the solutions to problems (9) and (23), respectively. Let $\mathbf{z} \in \mathbf{V}(\Omega), \mathbf{z} \neq \mathbf{0}$, and denote the quantity of interest by $\mathbf{L} \in \mathbf{V}'(\Omega)$. Moreover, let $s \in \mathbb{R}^+$. Then, the quantity $L(\mathbf{u} - \mathbf{z})$ can be bounded above and below :*

$$\eta_{\text{low}}(\mathbf{z}) \leq L(\mathbf{u} - \mathbf{z}) \leq \eta_{\text{upp}}(\mathbf{z}) \tag{48}$$

with

$$
\begin{aligned}
\eta_{\text{low}}(\mathbf{z}) \quad &\overset{\text{def}}{=} \quad \tfrac{1}{4}(\eta_{\text{low}}^+(s\mathbf{z} + s^{-1}\mathbf{w}^0))^2 - \tfrac{1}{4}(\eta_{\text{upp}}^-(s\mathbf{z} - s^{-1}\mathbf{w}^0))^2 \\
&\quad + \quad \mathcal{F}(\mathbf{w}^0) - \mathcal{B}(\mathbf{z}, \mathbf{w}^0),
\end{aligned}
\tag{49}
$$

and

$$
\begin{aligned}
\eta_{\text{upp}}(\mathbf{z}) \quad &\overset{\text{def}}{=} \quad \tfrac{1}{4}(\eta_{\text{upp}}^+(s\mathbf{z} + s^{-1}\mathbf{w}^0))^2 - \tfrac{1}{4}(\eta_{\text{low}}^-(s\mathbf{z} - s^{-1}\mathbf{w}^0))^2 \\
&\quad + \quad \mathcal{F}(\mathbf{w}^0) - \mathcal{B}(\mathbf{z}, \mathbf{w}^0),
\end{aligned}
\tag{50}
$$

and $\eta_{\text{upp}}^\pm(\mathbf{v})$ and $\eta_{\text{low}}^\pm(\mathbf{v})$, $\mathbf{v} \in \mathbf{V}(\Omega)$, are defined in (46) and (47), respectively.

Proof. We recall that $L(\mathbf{v}) = \mathcal{B}(\mathbf{v}, \mathbf{w}) \; \forall \; \mathbf{v} \in \mathbf{V}(\Omega)$. Therefore,

$$
\begin{aligned}
L(\mathbf{u} - \mathbf{z}) \quad &= \quad \mathcal{B}(\mathbf{u} - \mathbf{z}, \mathbf{w}) \\
&= \quad \mathcal{B}(\mathbf{u} - \mathbf{z}, \mathbf{w} - \mathbf{w}^0) + \mathcal{B}(\mathbf{u} - \mathbf{z}, \mathbf{w}^0) \\
&= \quad \mathcal{B}(s(\mathbf{u} - \mathbf{z}), s^{-1}(\mathbf{w} - \mathbf{w}^0)) + \mathcal{B}(\mathbf{u}, \mathbf{w}^0) - \mathcal{B}(\mathbf{z}, \mathbf{w}^0)
\end{aligned}
\tag{51}
$$

and since the energy norm $\|\cdot\|_{E(\Omega)}$ is derived from the bilinear form $\mathcal{B}(\cdot, \cdot)$,

$$
\begin{aligned}
L(\mathbf{u} - \mathbf{z}) \quad &= \quad \tfrac{1}{4}\|s(\mathbf{u} - \mathbf{z}) + s^{-1}(\mathbf{w} - \mathbf{w}^0)\|_{E(\Omega)}^2 \\
&\quad - \quad \tfrac{1}{4}\|s(\mathbf{u} - \mathbf{z}) - s^{-1}(\mathbf{w} - \mathbf{w}^0)\|_{E(\Omega)}^2 \\
&\quad + \quad \mathcal{B}(\mathbf{u}, \mathbf{w}^0) - \mathcal{B}(\mathbf{z}, \mathbf{w}^0) \\
&= \quad \tfrac{1}{4}\|(s\mathbf{u} + s^{-1}\mathbf{w}) - (s\mathbf{z} + s^{-1}\mathbf{w}^0)\|_{E(\Omega)}^2 \\
&\quad - \quad \tfrac{1}{4}\|(s\mathbf{u} - s^{-1}\mathbf{w}) - (s\mathbf{z} - s^{-1}\mathbf{w}^0)\|_{E(\Omega)}^2 \\
&\quad + \quad \mathcal{F}(\mathbf{w}^0) - \mathcal{B}(\mathbf{z}, \mathbf{w}^0).
\end{aligned}
\tag{52}
$$

Since the terms $\mathcal{F}(\mathbf{w}^0)$ and $\mathcal{B}(\mathbf{z}, \mathbf{w}^0)$ can be computed exactly, we need only bound the terms $\|(s\mathbf{u} \pm s^{-1}\mathbf{w}) - (s\mathbf{z} \pm s^{-1}\mathbf{w}^0)\|_{E(\Omega)}$. From (45), we have

$$\eta_{\text{low}}^\pm(s\mathbf{z} \pm s^{-1}\mathbf{w}^0) \leq \|(s\mathbf{u} \pm s^{-1}\mathbf{w}) - (s\mathbf{z} \pm s^{-1}\mathbf{w}^0)\|_{E(\Omega)} \leq \eta_{\text{upp}}^\pm(s\mathbf{z} \pm s^{-1}\mathbf{w}^0) \tag{53}$$

which concludes the proof. □

Note that the optimal value of the scaling factor s is now given by

$$s^* = \sqrt{\frac{\|\mathbf{w} - \mathbf{w}^0\|_{E(\Omega)}}{\|\mathbf{u} - \mathbf{z}\|_{E(\Omega)}}} \approx \sqrt{\frac{\bar{\zeta}_{\mathrm{upp}}}{\zeta_{\mathrm{upp}}^z}}. \tag{54}$$

Later, we will also use the following estimates of the quantity $L(\mathbf{u} - \mathbf{z})$:

$$
\begin{aligned}
L(\mathbf{u} - \mathbf{z}) \approx \eta_{\mathrm{est,upp}}^z \quad &\overset{\mathrm{def}}{=} \quad \tfrac{1}{4}(\eta_{\mathrm{upp}}^+(s\mathbf{z} + s^{-1}\mathbf{w}^0))^2 - \tfrac{1}{4}(\eta_{\mathrm{upp}}^-(s\mathbf{z} - s^{-1}\mathbf{w}^0))^2 \\
&+ \quad \mathcal{F}(\mathbf{w}^0) - \mathcal{B}(\mathbf{z}, \mathbf{w}^0),
\end{aligned}
\tag{55}
$$

and

$$
\begin{aligned}
L(\mathbf{u} - \mathbf{z}) \approx \eta_{\mathrm{est,low}}^z \quad &\overset{\mathrm{def}}{=} \quad \tfrac{1}{4}(\eta_{\mathrm{low}}^+(s\mathbf{z} + s^{-1}\mathbf{w}^0))^2 - \tfrac{1}{4}(\eta_{\mathrm{low}}^-(s\mathbf{z} - s^{-1}\mathbf{w}^0))^2 \\
&+ \quad \mathcal{F}(\mathbf{w}^0) - \mathcal{B}(\mathbf{z}, \mathbf{w}^0).
\end{aligned}
\tag{56}
$$

4 Goal-Oriented Adaptive Modeling

One way to overcome the loss of fine-scale information due to regularization techniques is to use the regularized solution as a starting point in a procedure that adaptively improves the quality of the solution. Such procedures are common in the context of finite elements where a coarse mesh solution is used as a starting point and is adaptively improved upon by refining the mesh. Here, we are concerned with adapting the model of the microstructure itself. We begin this section by describing a goal-oriented strategy for model adaptation for a given quantity of interest. We then present an algorithm based on this strategy.

4.1 Adaptive Modeling Strategy

Our strategy for adapting the material model based on modeling error in a quantity of interest $L \in \mathbf{V}'(\Omega)$ consists of :

1. Solution of the regularized problems (9) and (23) for $\mathbf{u}^0$ and $\mathbf{w}^0$, respectively

2. Estimation of the modeling error $L(\mathbf{u} - \mathbf{u}^0)$ in the quantity of interest using Theorem 3.1

3. If required, enhancement of the regularized solution $\mathbf{u}^0$ by taking into account the fine-scale material features over a "region of influence"

Let us elaborate further on the third part of our strategy. Suppose $\Omega_L \subset \Omega$ is determined to be (in a fashion to be described shortly) the region where the fine-scale elasticity tensor $\mathbf{E}$ most influences the quantity of interest L. We propose solving a problem on Ω_L with the regularized solution $\mathbf{u}^0$ providing the boundary conditions. More precisely, define

$$\Gamma_{L_t} \stackrel{\text{def}}{=} \partial \Omega_L \cap \Gamma_t, \quad \Gamma_{L_u} \stackrel{\text{def}}{=} \partial \Omega_L \setminus \Gamma_{L_t}. \tag{57}$$

Define the local function space on Ω_L as

$$\mathbf{V}(\Omega_L) = \left\{ \mathbf{v} \in \mathbf{V}(\Omega), \mathbf{v} = \mathbf{0} \text{ on } \Omega \setminus \overline{\Omega_L}, \mathbf{v}|_{\Gamma_{L_u}} = \mathbf{0} \right\}. \tag{58}$$

Next, an extension operator $\mathcal{E}_L : \mathbf{V}(\Omega_L) \to \mathbf{V}(\Omega)$ is introduced, defined by :

$$\mathbf{v}_L \in \mathbf{V}(\Omega_L), \ \mathcal{E}_L(\mathbf{v}_L) = \mathbf{v} \text{ such that } \mathbf{v}|_{\Omega_L} = \mathbf{v}_L, \mathbf{v}|_{\Omega \setminus \Omega_L} = \mathbf{0}. \tag{59}$$

The restriction of the regularized solution $\mathbf{u}^0$ to the domain of influence Ω_L is defined as $\mathbf{u}_L^0 : \mathbf{u}_L^0 \stackrel{\text{def}}{=} \mathbf{u}^0|_{\Omega_L}$. Then $\tilde{\mathbf{u}}_L$ is sought as the solution to the following weak boundary value problem :

$$\boxed{\begin{array}{l} \text{Find } \tilde{\mathbf{u}}_L \in \{\mathbf{u}_L^0\} + \mathbf{V}(\Omega_L) \text{ such that} \\ \mathcal{B}_L(\tilde{\mathbf{u}}_L, \mathbf{v}_L) = \mathcal{F}_L(\mathbf{v}_L) \quad \forall \, \mathbf{v}_L \in \mathbf{V}(\Omega_L), \end{array}} \tag{60}$$

where the bilinear and linear forms are defined as

$$\mathcal{B}_L(\tilde{\mathbf{u}}_L, \mathbf{v}_L) \stackrel{\text{def}}{=} \int_{\Omega_L} \boldsymbol{\nabla} \mathbf{v}_L : \mathbf{E} \, \boldsymbol{\nabla} \tilde{\mathbf{u}}_L \, \mathrm{d}\mathbf{x}, \tag{61}$$

and

$$\mathcal{F}_L(\mathbf{v}_L) \stackrel{\text{def}}{=} \int_{\Omega_L} \mathbf{f} \cdot \mathbf{v}_L \, \mathrm{d}\mathbf{x} + \int_{\Gamma_{L_t}} \mathbf{t} \cdot \mathbf{v}_L \, \mathrm{d}\mathbf{s}, \tag{62}$$

respectively. Thus, $\tilde{\mathbf{u}}_L$ is a perturbation on Ω_L that takes into account the fine-scale microstructure. Moreover, it equals the primal regularized solution $\mathbf{u}^0$ on the Γ_{L_u} portion of its boundary. Using the extension operator introduced earlier, we arrive at a *locally enhanced* function $\tilde{\mathbf{u}} \in \mathbf{V}(\Omega)$ defined as :

$$\tilde{\mathbf{u}} \stackrel{\text{def}}{=} \mathbf{u}^0 + \mathcal{E}_L(\tilde{\mathbf{u}}_L - \mathbf{u}_L^0). \tag{63}$$

We now make two observations :

- The locally enhanced solution $\tilde{\mathbf{u}} \in \mathbf{V}(\Omega)$ is an admissible function and satisfies the kinematic constraint $\tilde{\mathbf{u}}|_{\Gamma_u} = \mathbf{0}$, even though it is not the solution to a global problem posed on Ω.

- The modeling error in the quantity of interest L corresponding to the perturbed solution is $L(\mathbf{u}) - L(\tilde{\mathbf{u}}) = L(\mathbf{u} - \tilde{\mathbf{u}})$. This quantity can be bounded above and below using Theorem 3.2.

We now propose a technique to determine the "domain of influence" Ω_L. We consider a non-overlapping partition $\mathcal{P}$ of the domain Ω into cells Θ_k, $1 \leq k \leq N(\mathcal{P})$, where $N(\mathcal{P})$ is the total number of cells in the partition. Define

$$
\begin{aligned}
\zeta_{k,\mathrm{upp}} &\stackrel{\mathrm{def}}{=} \left\{ \int_{\Theta_k} \mathcal{I}_0 \boldsymbol{\nabla} \mathbf{u}^0 : \mathbf{E}\, \mathcal{I}_0 \boldsymbol{\nabla} \mathbf{u}^0 \,\mathrm{d}\mathbf{x} \right\}^{\frac{1}{2}} \\
\bar{\zeta}_{k,\mathrm{upp}} &\stackrel{\mathrm{def}}{=} \left\{ \int_{\Theta_k} \mathcal{I}_0 \boldsymbol{\nabla} \mathbf{w}^0 : \mathbf{E}\, \mathcal{I}_0 \boldsymbol{\nabla} \mathbf{w}^0 \,\mathrm{d}\mathbf{x} \right\}^{\frac{1}{2}},
\end{aligned}
\tag{64}
$$

and note that

$$
\zeta_{\mathrm{upp}}^2 = \sum_{k=1}^{N(\mathcal{P})} \zeta_{k,\mathrm{upp}}^2, \quad \bar{\zeta}_{\mathrm{upp}}^2 = \sum_{k=1}^{N(\mathcal{P})} \bar{\zeta}_{k,\mathrm{upp}}^2,
\tag{65}
$$

where ζ_{upp} and $\bar{\zeta}_{\mathrm{upp}}$ were introduced in (15) and (27), respectively. Next, note that the proof of Theorem 3.1 (see [5]) is based on the decomposition

$$
L(\mathbf{e}^0) = \mathcal{B}(\mathbf{e}^0, \bar{\mathbf{e}}^0) + \mathcal{B}(\mathbf{e}^0, \mathbf{w}^0),
\tag{66}
$$

which implies that

$$
|L(\mathbf{e}^0)| \leq \beta \stackrel{\mathrm{def}}{=} \zeta_{\mathrm{upp}} \bar{\zeta}_{\mathrm{upp}} + \zeta_{\mathrm{upp}} \|\mathbf{w}^0\|_{E(\Omega)}.
\tag{67}
$$

This suggests that the cells k in which the quantity

$$
\beta_k \stackrel{\mathrm{def}}{=} \zeta_{k,\mathrm{upp}} \bar{\zeta}_{k,\mathrm{upp}} + \zeta_{k,\mathrm{upp}} \|\mathbf{w}^0\|_{E(\Theta_k)}
\tag{68}
$$

exceeds a tolerance can be picked to constitute the domain of influence Ω_L.

4.2   The Goal-Oriented Adaptive Local Solution Algorithm (GOALS)

We begin by considering quantities of interest of the type

$$L(\mathbf{v}) = \int_\omega l(\mathbf{v}) \, \mathrm{d}\mathbf{x}, \ \ \omega \subset \Omega, \tag{69}$$

where l is a linear map : $l : \mathbf{V}(\Omega) \to L^1_{\mathrm{loc}}(\Omega)$. Our algorithm can be easily modified to accommodate quantities of interest of other types. The GOALS algorithm can now be stated as follows :

Step 1. Initialization. Given the initial data Ω, Γ_u, Γ_t, $\mathbf{E}$, $\mathbf{f}$ and $\mathbf{t}$, construct a non-overlapping partition of the domain $\mathcal{P} = \{\Theta_k\}, k = 1, 2 \ldots N(\mathcal{P})$. Specify error tolerance parameters α_{TOL} and δ_{TOL}, $0 < \delta_{\mathrm{TOL}} < 1$.

Step 2. Regularization. Compute the homogenized elasticity tensor $\mathbf{E}^0$. Solve the primal regularized problem (9) for $\mathbf{u}^0$ and the adjoint regularized problem (23) for $\mathbf{w}^0$.

Step 3. Modeling Error Estimation. Compute error indicators ζ_k, $\bar{\zeta}_k$ and β_k for $1 \leq k \leq N(\mathcal{P})$, using (64) and (68). Estimate the modeling error in the quantity of interest using Theorem 3.1. Denote this estimate by η_{est}.

Step 4. Tolerance Test. If $\eta_{\mathrm{est}} \leq \alpha_{\mathrm{TOL}} \times L(\mathbf{u}^0)$, STOP.

Step 5. Domain of Influence. Determine initial guess for "domain of influence" Ω_L as all the cells that intersect ω, the region over which the quantity of interest is defined :

$$\overline{\Omega_L} = \overline{\cup_{j \in \mathcal{J}} \Theta_j} \quad \mathcal{J} \stackrel{\mathrm{def}}{=} \{j : \Theta_j \cap \omega \neq \emptyset\} . \tag{70}$$

Compute the quantities $\zeta_L, \bar{\zeta}_L$, and β_L :

$$\zeta_L \stackrel{\mathrm{def}}{=} \left\{ \sum_{k \in \mathcal{J}} \zeta_{k,\mathrm{upp}}^2 \right\}^{\frac{1}{2}}, \ \bar{\zeta}_L \stackrel{\mathrm{def}}{=} \left\{ \sum_{k \in \mathcal{J}} \bar{\zeta}_{k,\mathrm{upp}}^2 \right\}^{\frac{1}{2}}, \ \beta_L \stackrel{\mathrm{def}}{=} \zeta_L \bar{\zeta}_L + \zeta_L \|\mathbf{w}^0\|_{E(\Omega_L)} \tag{71}$$

Step 6. Update Domain of Influence. Determine the "bad neighbors" of Ω_L, i.e., if $\beta_i > \delta_{\mathrm{TOL}} \times \beta_L$, mark Θ_i as bad and update Ω_L :

$$\Omega_L \leftarrow \Omega_L \cup \{ \text{ bad neighbors } \} . \tag{72}$$

Update the quantities $\zeta_L, \bar{\zeta}_L$, and β_L.

Step 7. Solution of Local Problem. Solve local problem (60) on Ω_L for $\tilde{\mathbf{u}}_L$. Construct the locally enhanced solution $\tilde{\mathbf{u}} \in \mathbf{V}(\Omega)$ using (63).

Step 8. Estimate Modeling Error. Estimate the modeling error $L(\mathbf{u} - \tilde{\mathbf{u}})$ using Theorem 3.2 and denote the estimate by η_{est}. If $\eta_{\mathrm{est}} \leq \alpha_{\mathrm{TOL}} \times L(\tilde{\mathbf{u}})$, STOP. Else, GOTO Step 6.

In many applications, the decay of local effects may be very fast, meaning that Ω_L is often small in comparison with Ω. However, cases can be anticipated, such as composites with fiber reinforcements, where decay rates are small and relatively large domains of influence may be needed to attain the target accuracies.

5   Numerical Experiment

To illustrate the adaptive modeling strategy proposed earlier, we consider a partially loaded 2-phase composite material in which the matrix material and the cylindrical inclusions are both isotropic. The volume fraction of the inclusions is taken to be 0.3 and they are randomly dispersed in the matrix material as shown in Figure 1. The material properties are taken to be ($E = 100.0MPa, \nu = 0.2$) for the matrix material and ($E = 1000.0MPa, \nu = 0.2$) for the inclusions, where E is the Young's modulus and ν is the Poisson's ratio. Plane strain conditions are assumed to hold.
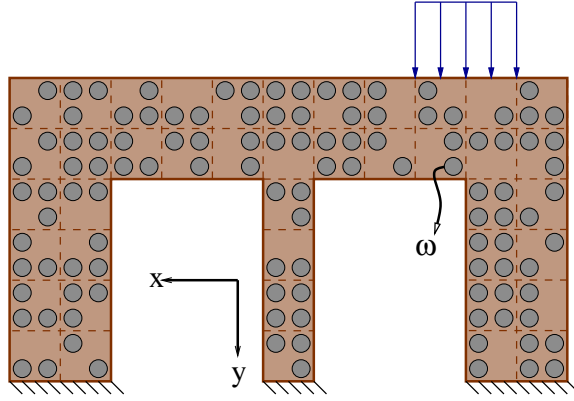
Figure 1: Schematic of the composite body considered. Dashed lines indicate the partitioning of the domain into cells.

We are interested in determining a material model that accurately predicts the following quantity of interest :

$$L(\mathbf{v}) = \frac{1}{|\omega|} \int_\omega \sigma_{11}(\mathbf{v})\,\mathrm{d}\mathbf{x} = \frac{1}{|\omega|} \int_\omega \left(C_1 \frac{\partial v_1}{\partial x} + C_2 \frac{\partial v_2}{\partial y} \right)\,\mathrm{d}\mathbf{x}, \qquad (73)$$

where ω is the region occupied by the inclusion indicated in Figure 1. This quantity of interest is the average of the σ_{11} component of the stress tensor on the inclusion ω (with appropriate material constants C_1 and C_2).

In order to evaluate the accuracy and effectivity of various bounds, we compute reference fine-scale solutions $\mathbf{u}$ and $\mathbf{w}$ using well resolved h-p meshes and the h-p adaptive finite
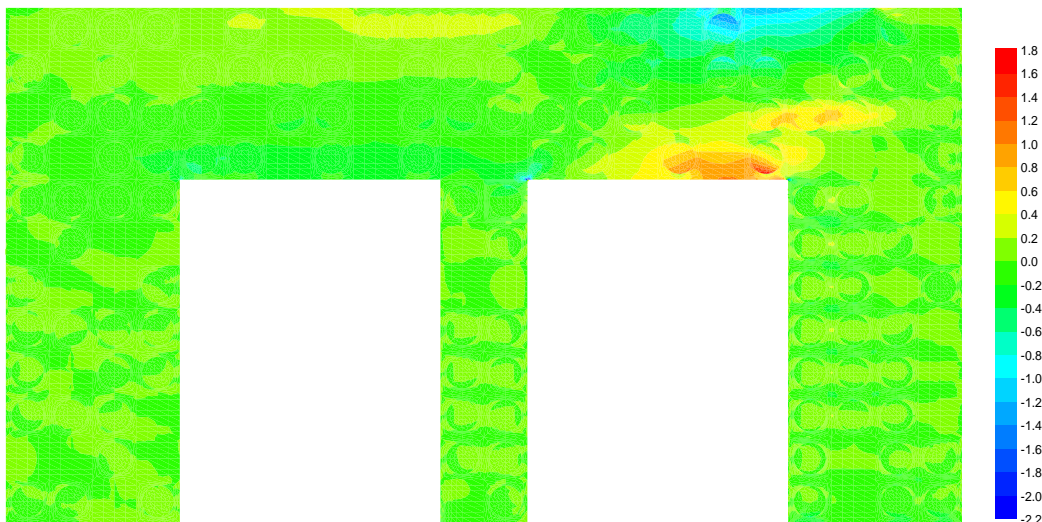
Figure 2: The σ_{11} component of the stress field $\boldsymbol{\sigma}(\mathbf{u})$.

element code ProPHLEX$^{\text{TM}}$ [2]. For instance, the h-p mesh used in computing the primal fine-scale solution $\mathbf{u}$ has $111,000$ degrees of freedom. The σ_{11} component of the stress field $\boldsymbol{\sigma}(\mathbf{u})$ is shown in Figure 2.

The domain is partitioned into $N(\mathcal{P}) = 42$ cells as indicated by the dashed lines in Figure 1 (Step 1 of the GOALS algorithm). Because of the lack of microstructural periodicity, the homogenized properties of the domain are taken to be the average of the Hashin-Shtrikman upper and lower bounds [3] (Step 2). Next, the homogenized problems (9) and (23) are solved accurately to obtain the homogenized solutions $\mathbf{u}^0$ and $\mathbf{w}^0$, respectively. Again, this is done using the h-p adaptive finite element code ProPHLEX$^{\text{TM}}$.

As the next step in the GOALS algorithm, the modeling error indicators $\zeta_{k,\text{upp}}$, $\bar{\zeta}_{k,\text{upp}}$, and β_k are computed using (64) and (68). In Figures 3, 4, and 5, we show the normalized quantities ζ_k, $\bar{\zeta}_k$, and β_k, $1 \leq k \leq 42$, respectively. A major difference between the distribution of the primal and the adjoint error indicators is that the primal indicators are global in nature whereas the adjoint indicators are highly local. In fact, only two cells contribute substantially to the adjoint modeling error estimate $\bar{\zeta}_{\text{upp}}$. This localized behavior is also seen in the distribution of the error indicators β_k.

To assess the quality of the error bounds and estimates computed in this step of the GOALS algorithm, we use the notion of an *effectivity index*. For a given error estimate, the effectivity index is defined as the ratio of the estimated error to the true error. In our case, we compute the "true error" using the reference solutions $\mathbf{u}$ and $\mathbf{w}$. The closer the effectivity index is to unity, the better the quality of the estimate. Thus, the effectivity index of the upper bound on the homogenization error ζ_{upp} introduced in (15) is
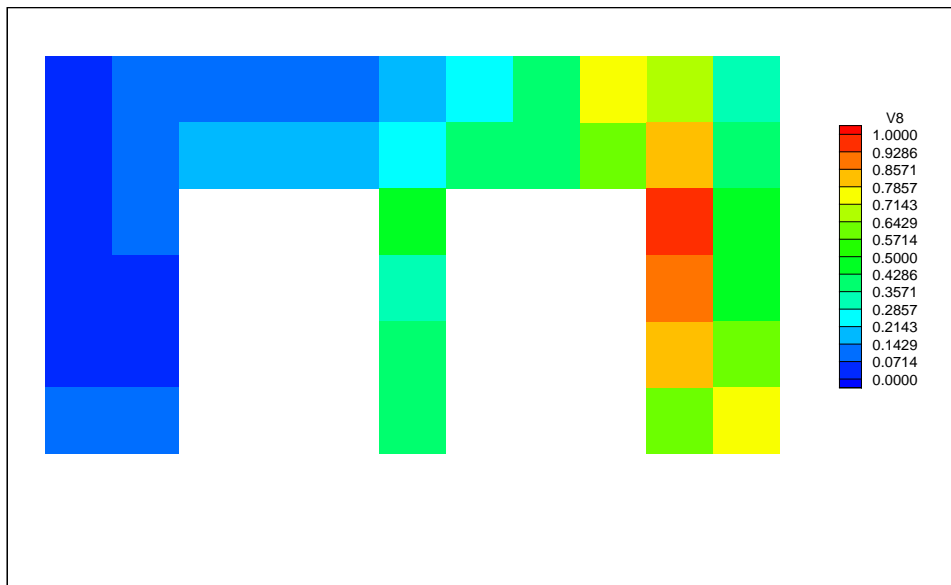
Figure 3: Distribution of the quantity $\zeta_{k,\mathrm{upp}}$ normalized with respect to the maximum.
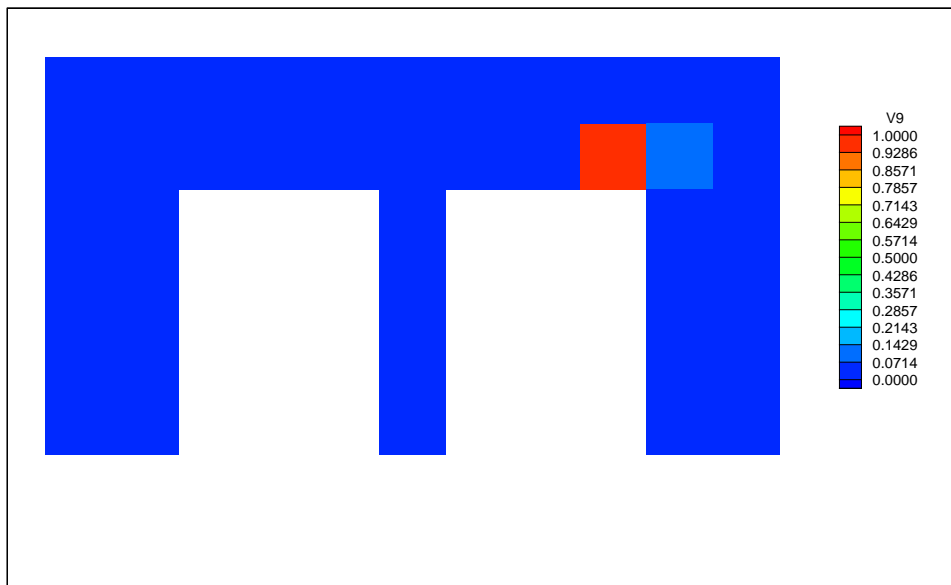

Figure 4: Distribution of the quantity $\bar{\zeta}_{k,\mathrm{upp}}$ normalized with respect to the maximum.

$\zeta_{\mathrm{upp}}/\|\mathbf{u} - \mathbf{u}^0\|_{E(\Omega)}$. First, the effectivity indices of the estimates corresponding to the primal problem are shown Table 1. We see that the upper bound ζ_{upp} is very close to true homogenization error $\|\mathbf{u} - \mathbf{u}^0\|_{E(\Omega)}$, whereas the lower bound is inefficient.

The effectivity indices of the estimates associated with the adjoint problem are next shown
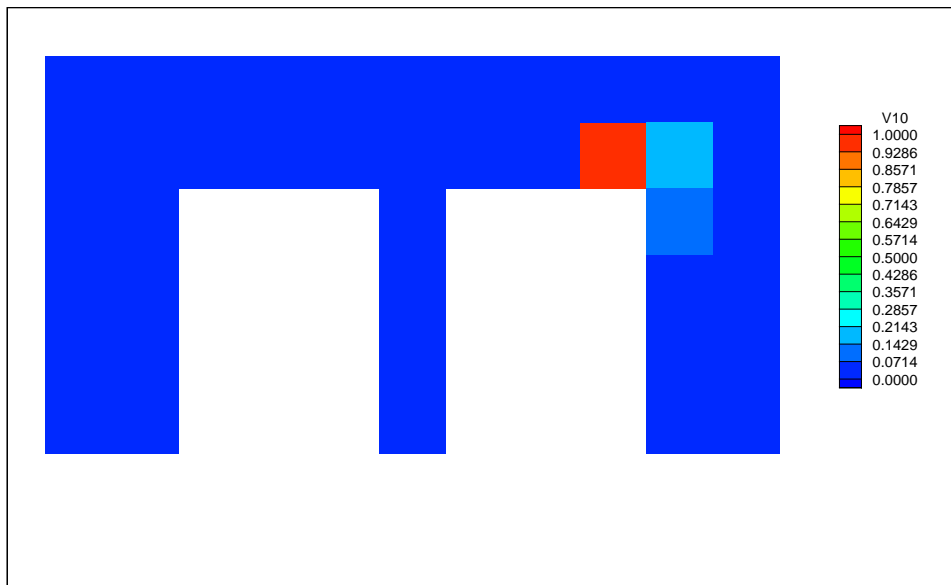
Figure 5: Distribution of the quantity β_k normalized with respect to the maximum.

$\dfrac{\zeta_{\mathrm{upp}}}{\|\mathbf{u} - \mathbf{u}^0\|_{E(\Omega)}}$	1.0848
$\dfrac{\zeta_{\mathrm{low}}}{\|\mathbf{u} - \mathbf{u}^0\|_{E(\Omega)}}$	0.4966

Table 1: Effectivity indices of the estimates associated with the primal problem.

in Table 2. For the adjoint problem, both the upper and lower bounds on $\|\mathbf{w} - \mathbf{w}^0\|_{E(\Omega)}$ are seen to be accurate. The bounds η_{upp} and η_{low} on the modeling error in the quantity of interest are far from unity as expected; for a detailed analysis of the accuracy of these bounds, see [5]. The arithmetic average of these bounds, denoted by η_{av}, and the estimates of the modeling error $\eta_{\mathrm{est,low}}$ and $\eta_{\mathrm{est,upp}}$ are much more reasonable and can be used to drive the adaptive process.

The relative modeling error in the quantity of interest L, defined as $L(\mathbf{u} - \mathbf{u}^0)/L(\mathbf{u})$ is found to be 351%. In order to reduce this error, we adapt the material model as follows. The cell containing the inclusion ω is chosen as an initial guess for the domain of influence Ω_L. Note that this is the cell with the largest error indicator β_k. The local problem (60) is solved on this cell using a well-resolved h-p adaptive mesh, and the enhanced solution $\tilde{\mathbf{u}}$ is constructed. The error in the quantity of interest is now drastically reduced and we find $L(\mathbf{u} - \tilde{\mathbf{u}})/L(\mathbf{u}) = 6.7\%$.

The material model is further adapted by choosing Ω_L to be the union of the three cells

$\dfrac{\bar{\zeta}_{\text{upp}}}{\|\mathbf{w} - \mathbf{w}^0\|_{E(\Omega)}}$	1.1191
$\dfrac{\bar{\zeta}_{\text{low}}}{\|\mathbf{w} - \mathbf{w}^0\|_{E(\Omega)}}$	0.9979
$\dfrac{\eta_{\text{upp}}}{L(\mathbf{e}^0)}$	-7.0692
$\dfrac{\eta_{\text{low}}}{L(\mathbf{e}^0)}$	8.8310
$\dfrac{\eta_{\text{av}}}{L(\mathbf{e}^0)}$	0.8809
$\dfrac{\eta_{\text{est,low}}}{L(\mathbf{e}^0)}$	1.0574
$\dfrac{\eta_{\text{est,upp}}}{L(\mathbf{e}^0)}$	0.7044

Table 2: Effectivity indices of the estimates associated with the adjoint problem corresponding to the quantity of interest L.

with the largest β_ks. This leads to an L-shaped domain (see Fig. 5). The process of solving a local problem, as described above, is repeated and the enhanced solution $\tilde{\mathbf{u}}$ is constructed. Now, we find $L(\mathbf{u} - \tilde{\mathbf{u}})/L(\mathbf{u}) = 0.9\%$.

Thus, the material model required to predict the quantity of interest L to within 1% consists of the fine-scale features in just three cells of the partition, and the homogenized material elsewhere.

6   Summary and Conclusions

The concept of adaptive modeling of materials makes no assumptions about the existence of Representative Volume Elements (RVEs) or the periodicity of microstructure, as is usual in the traditional analysis of composites. Using regularization as part of a larger algorithm, adaptive modeling attempts to deliver material models that satisfy preset accuracy requirements.

In this work, we present a new theory for the *goal-oriented* adaptive modeling of heterogeneous materials, and an algorithm for adapting material models based on our theory of local modeling error estimation. Preliminary numerical examples demonstrate the advantages that such modeling techniques have over traditional methods. Extensive numerical experiments, details of a parallel computational infrastructure for the adaptive modeling of heterogeneous materials, and the incorporation of imaging technology into such

analyses are subjects to be addressed in future work.

References

[1] Ainsworth, M. and Oden, J. T. "A Posteriori Error Estimation in Finite Element Analysis". *Comp. Meth. Applied Mech. Engng.*, 142 (1997) 1–88.

[2] Computational Mechanics Company, Inc., Austin, TX. *ProPHLEX User Manual for Version 2.0*, 1996.

[3] Hashin, Z. "Analysis of Composite Materials, A Survey". *J. Appl. Mech.*, 50 (1983) 481–505.

[4] Jikov, V. V., Kozlov, S. M., and Oleinik, O. A. *Homogenization of Differential Operators and Integral Functionals*. Springer-Verlag, Heidelberg, 1994.

[5] Oden, J. T. and Vemaganti, K. "Adaptive Modeling of Composite Structures : Modeling Error Estimation". Technical Report TR 1999-11, Texas Institute for Computational and Applied Mathematics, Austin, Texas, 1999.

[6] Oden, J. T., Vemaganti, K., and Moës, N. "Hierarchical Modeling of Heterogeneous Solids". *Comp. Meth. Applied Mech. Engng.*, 172 (1999) 3–25.

[7] Oden, J. T. and Zohdi, T. I. "Analysis and Adaptive Modeling of Highly Heterogeneous Elastic Structures". *Comp. Meth. Applied Mech. Engng.*, 148 (1997) 367–391.

[8] Prudhomme, S. and Oden, J. T. "On goal-Oriented Error Estimation for Elliptic Problems : Application to the Control of Pointwise Errors". *Comp. Meth. Applied Mech. Engng.*, 176 (1999) 313–331.

[9] Sanchez-Palencia, E. *Non-homogeneous Media and Vibration Theory*. Number 127 in Lecture Notes in Physics. Springer-Verlag, Berlin, 1980.

[10] Vemaganti, K. and Oden, J. T. "Estimation of Local Modeling Error and Goal-Oriented Adaptive Modeling of Heterogeneous Materials; Part II : A Computational Environment for Adaptive Modeling of Heterogeneous Elastic Solids". In preparation.

[11] Zohdi, T. I., Oden, J. T., and Rodin, G. J. "Hierarchical Modeling of Heterogeneous Bodies". *Comp. Meth. Applied Mech. Engng.*, 138 (1996) 273–298.